Powder Technology 208 (2011) 643–656

Contents lists available at ScienceDirect

Powder Technology

journal homepage: www.elsevier.com/locate/powtec

# Comparison of the multi-sphere and polyhedral approach to simulate non-spherical particles within the discrete element method: Influence on temporal force evolution for multiple contacts

D. Höhner *, S. Wirtz, H. Kruggel-Emden, V. Scherer

*Ruhr-University of Bochum, Department of Energy Plant Technology, Germany*

ARTICLE INFO

*Article history:*
Received 6 August 2010
Received in revised form 6 December 2010
Accepted 8 January 2011
Available online 20 January 2011

*Keywords:*
Discrete element method
Multiple contacts
Multi-sphere approach
Polyhedra

ABSTRACT

In this paper a multi-sphere as well as a polyhedral approach is investigated as method of shape-approximation within the discrete element method. The two approaches are compared against each other using an ellipsoidal particle impacting on a flat wall as a reference scenario. In general it is shown that there is a non-negligible effect of shape approximation on the temporal force evolution in normal and tangential direction. The occurrence of multiple contacts between the particles when approximated by a multi-sphere or a polyhedral approach is detected as a main source of differences between the exact solution and the solution of the approximated particles. A method to account for these effects is provided in order to increase the accuracy when complex particle shapes are used. Moreover the effect of shape-approximation accuracy on the accuracy of the results is investigated. For both approximation procedures higher accuracy levels in terms of particle shape representation do not automatically lead to more accurate results for normal and tangential forces in the investigated collision scenarios. It will be shown that the effects of a more accurate ellipsoid-surface approximation and higher numbers of contact points influence the quality of the results in opposite directions.



## 1. Introduction

Most discrete element codes represent particle shape with discs (in 2D) or spheres (in 3D). The advantage of using discs or spheres to represent particle shape is their simplicity especially in terms of inter-particle contact detection. Moreover the contact force models for contacting spheres and spheres contacting flat walls are well known [1–4]. Since discrete element simulations usually involve large numbers of discrete elements, minimizing computing time is a very important aspect. While spheres are easy to handle in a DEM-Code, they show a different mechanical behaviour on the single grain level as well as in larger assemblies compared to the actual particle behaviour in most application areas [5,6]. For example interlocking of particles cannot be simulated using spherical shape representation. Therefore the physical meaning of results obtained from these simulations is questionable [7].

Representation of the particle shape is one of the key challenges of DEM simulations [8]. In order to obtain more realistic particle behaviour other particle shape approximations have been introduced into the discrete element method. Basically two different approaches can be recognized: the single-particle approach and the clustered-particle approach. In a single particle approach the particle is a single particle of complicated geometry such as an ellipsoid [9,10], superquadric [11,12] or polyhedron [13–15]. In the clustered particle approach smaller body elements such as spheres are connected in order to form a clustered particle of complex shape [7,16,17]. A broad overview of possible particle shape representations in the discrete element method can be found in Hogue [18] as well as Latham and Munjiza [5].

Elliptical particles are probably the most widely used non-spherical smooth particle shape in DEM simulations [8]. The usage of ellipses (2D) and ellipsoids (3D) decreases the inherent rolling tendency of spherical particles which is considered as one of the major causes of deviation of DEM simulations from realistic particle behaviour [19]. Contact detection between elliptical and ellipsoidal particles usually involves a numerical calculation of polynomial roots which can be very time-consuming depending on the applied numerical algorithm and the chosen initial value of the iteration. Contact detection schemes for elliptical and/or ellipsoidal particles were presented i.e. by Lin and Ng [9,20], Dziugys and Peters [21], Ouadfel and Rothenburg [10] as well as Rothenburg and Bathurst [22]. Note that the shape approximation with ellipsoids is not further studied in the scope of the current paper but the contact between an ellipsoid and a flat wall is used as reference scenario for the multi-sphere and the polyhedral approach (see Section 5).

Another interesting approach to implement more complex particles is the usage of polyhedral body shapes. Polyhedral particles

* Corresponding author.
*E-mail address:* dominik.hoehner@leat.ruhr-uni-bochum.de (D. Höhner).

0032-5910/$ – see front matter © 2011 Elsevier B.V. All rights reserved.
doi:10.1016/j.powtec.2011.01.003

in general as introduced by Cundall [13] are widely used in DEM simulations. Various methods for contact detection between polyhedral bodies exist and can be found in Refs. [13–15,37]. The question of how contact forces between two colliding polyhedral bodies are calculated is still not completely answered. In some algorithms only the vertices of the polyhedral surface are checked for contact with another polyhedra [15,23] while in others contacts are differentiated among different contact types [13,24]. The advantage of polyhedral particles is that a wide variety of complex and asymmetrical particle shapes can be simulated resulting in more realistic discrete element simulations.

The composite-particle or clustered-particle approach is basically restricted to multi-sphere models [7,16,17] which were introduced by Favier et al. [25] and Abbaspour-Fard [26]. In the multi-sphere model the single particle is represented by a composition of connected spheres which may vary in size and even overlap each other [7,27]. This shape representation algorithm can be easily implemented and shows efficient contact detection because it employs a sphere–sphere contact detection algorithm for irregular shaped objects [28]. Moreover it is suitable for modelling asymmetrically shaped objects. Once a model particle is created, the relative distances between the component spheres remain fixed throughout the simulation so that the generated clustered particle remains a rigid body.

While plenty of studies about the contact detection procedures between particles of above described approaches exist, the influence of shape approximation on the contact force resolution is still a consequence that is not adequately addressed. Especially the effect of multiple contacts during a collision as induced by more complex particle representations is only to some degree covered in scientific literature [7,8,16,28]. Also the authors are not aware of publications which compare the influence of multi-sphere and polyhedral approaches on temporal force evolution.

Section 2 of this paper illustrates the force schemes in normal and tangential direction which are applied for the following numerical simulations of a single particle impacting a stationary flat wall. In Section 3 the multi-sphere method and the application of polyhedral bodies as two commonly used approximation schemes to approximate real particle shapes are presented. In order to demonstrate the occurrence of multiple contact collisions Section 4 investigates a spherical-particle approximated with the multi-sphere method impacting a stationary flat wall. The influence of multiple contacts on the resulting contact forces is demonstrated by comparing the solution to the reference solution of a perfect single sphere in the same collision scenario. A procedure to decrease the artificial effect of multiple contacts on the force calculation is proposed at the end of Section 4 as well as its efficiency is demonstrated. In Section 5 a more practical example of shape-approximation with the multi-sphere method and the polyhedron-based approach is investigated. The results of different collision scenarios for the two approximation schemes are compared with each other and with the reference solution of an ellipsoid impacting on a flat wall. The examination of different approximation accuracies illustrates its effect as well as the effect of multiple contacts on the accuracy of the results obtained.

## 2. Force laws applied

The discrete element method allows particles to overlap and computes the resulting contact forces as a function of the particle overlap. The particle overlap leads to the compression of a spring in normal and tangential direction. An overview over force schemes for the normal and tangential contact direction is given by Kruggel-Emden [1–3] as well as Di Renzo and Di Maio [4].

One of the most frequently employed normal force laws in DEM-simulations is the linear viscoelastic spring dashpot model [29–31]. The normal force $F^n$ consists of two parts: the elastic component models elastic repulsion, while the dissipative component accounts for the dissipation of energy during the collision. The force law is called linear because of its linear dependency on the overlap of the colliding discrete elements as well as the relative velocity between the contact partners. Fig. 1 shows a schematic of the linear viscoelastic spring dashpot model.

The normal force can be determined as [29,32]

$$F^n = F^{n,el} + F^{n,diss} = -k^n \cdot \xi^n - \gamma^n \cdot \dot{\xi}^n \tag{1}$$

With

$k^n$ Stiffness of a normal linear spring
$\gamma^n$ Constant of a velocity proportional dashpot
$\xi^n$ Normal overlap of two contacting discrete elements
$\dot{\xi}^n$ Relative normal velocity of two contacting discrete elements

Also for the tangential direction linear models are often applied [33,34] (Fig. 2). The earliest approach was proposed by Cundall and Strack [35]. In their model, the tangential contact force is calculated according to a linear elastic spring unless the related Coulomb force is exceeded. The force of the tangential spring can be determined as

$$F^{t,tspg} = -k^t \cdot \xi^t \cdot sign\left(\xi^t\right) \tag{2}$$

while the Coulomb force can be determined as

$$F^{t,coul} = -\mu \cdot F^n \cdot sign\left(\xi^t\right). \tag{3}$$

Following for the tangential contact force

$$F^t = -min\left(\left|k^t \cdot \xi^t\right|, \left|\mu \cdot F^n\right|\right) \cdot sign\left(\xi^t\right) \tag{4}$$

With

$k^t$ Stiffness of a tangential linear spring
$\xi^t$ Tangential overlap of two contacting discrete elements
$\mu$ Friction coefficient

The tangential overlap $\xi_i^t$ in iteration step $i$ can be incrementally determined as

$$\xi_i^t = v_i^t \cdot dt + \xi_{i-1}^t \tag{5}$$

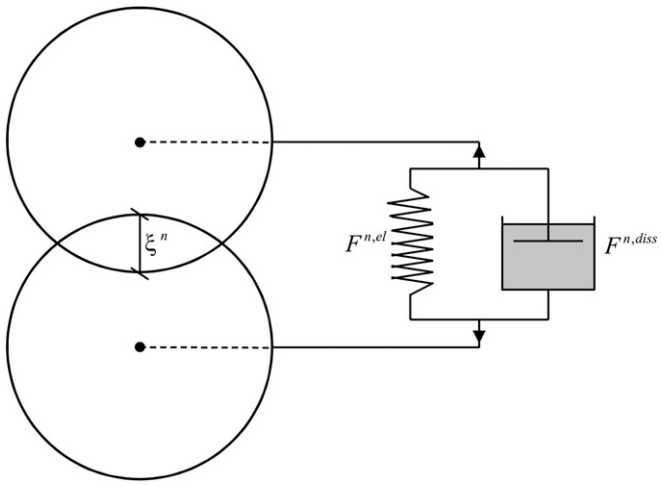


**Fig. 1.** Schematic of the normal linear viscoleastic spring dashpot model.

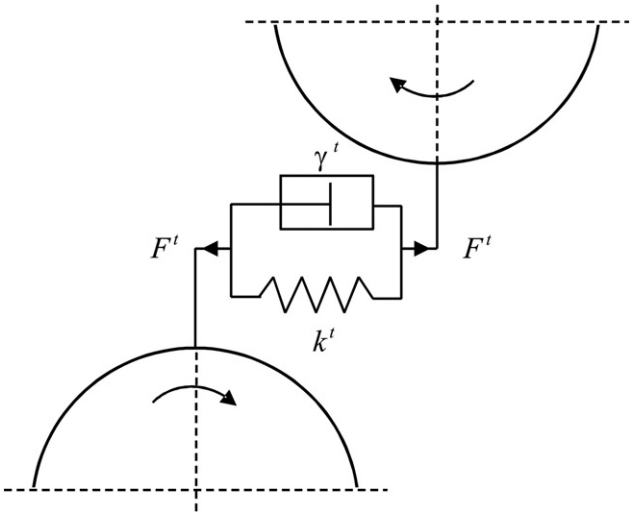


**Fig. 2.** Schematic of the tangential linear viscoelastic spring dashpot model.

**Table 1**
Force law parameters applied for the simulation.

| Stiffness of the normal spring [kN/mm] | Damping coefficient [kg/s] | Stiffness of the tangential spring [kN/mm] | Friction coefficient [−] | Density (sphere) [kg/m³] |
|---|---|---|---|---|
| 125 | 1.0 | 100 | 0.18 | 3.900 |

With

$v_i^t$ Tangential relative velocity of two contacting discrete elements
$dt$ Time step of the DEM-iteration
$\xi_{i-1}^t$ Tangential overlap of the previous DEM-iteration step

The combination of the force laws briefly outlined above is employed in the following described DEM-simulations.

All simulations investigated in this paper are carried out with the same set of parameters as listed in Table 1.

## 3. Particle shape approximation

For the purpose of comparison Fig. 3 shows a sphere-approximation conducted with a) a multi-sphere approach and b) a polyhedron-based approach for different numbers of inscribed spheres or triangular surface elements, i.e. different levels of accuracy.

The following section gives a brief overview on both approximation methods mentioned.

### 3.1. Multi-sphere approach

In the multi-sphere model a single particle is represented by a set of connected spheres which are inscribed into the real particle shape (Fig. 4) such that at each contact point of sphere and real body a tangential plane can be constructed. The component spheres forming a cluster-particle may otherwise vary in size and even overlap each other [7,27].

In contrast to spherical particles the orientation of any more complexly shaped particle has to be accounted for. Therefore apart from the global frame of reference an additional body-fixed frame is required to describe translational and rotational body motion of the clustered particle (CP). The location of the component spheres (CSP) can be determined as

$$\vec{x}_{j,CSP} = \vec{x}_{CP} + M_P \cdot \vec{r}_j \tag{6}$$

With

$M_P$ Rotational matrix converting vectors from the body-fixed frame to the global coordinate system
$\vec{r}_j$ Vector from the clustered particle's centre of gravity to the centre of gravity of component sphere $j$

Analogously the velocity of the component spheres can be determined as

$$\dot{\vec{x}}_{j,CSP} = \dot{\vec{x}}_{CP} + M_P\left(\vec{\omega}_{CP} \times \vec{r}_j\right) \tag{7}$$

With

$\vec{\omega}_{CP}$ Rotational velocity of the clustered particle

Contact detection for a particle approximated with the multi-sphere approach is analogous to a spherical particle. Each component sphere of particle A is checked for contact against each component sphere of particle B or in the case of a particle-wall contact each component sphere is checked for contact against the wall. The overlap is determined for each component sphere the same way as conducted for spherical particles.

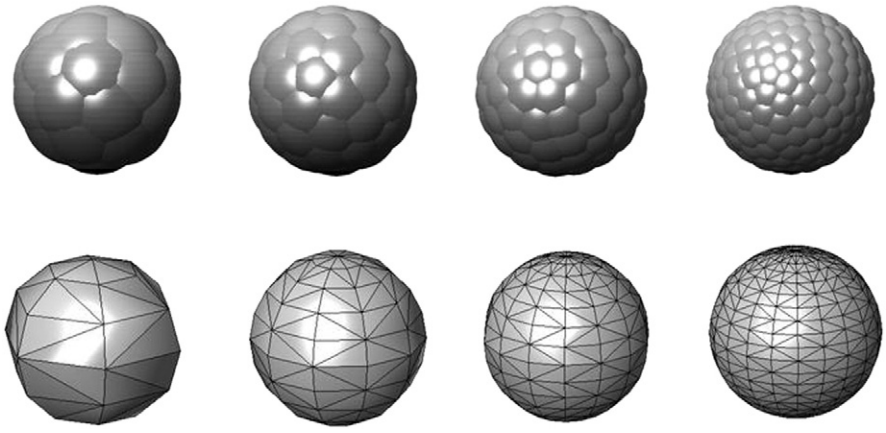

**Fig. 3.** Sphere approximated with a multi-sphere approach and a polyhedron with triangular surface elements for different levels of accuracy.

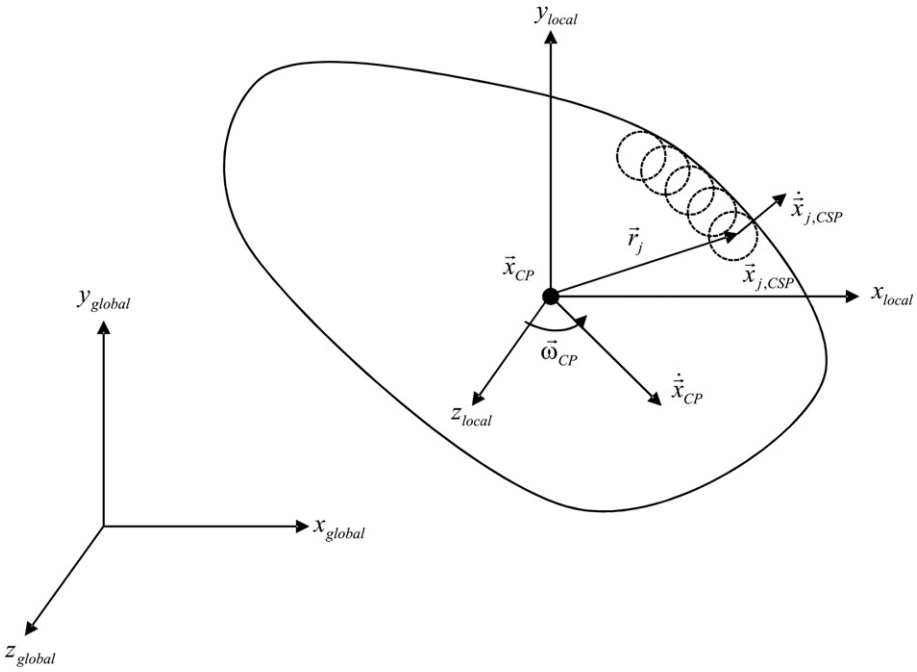


**Fig. 4.** Relevant position and velocity vectors of a clustered particle approximated with a multi-sphere approach.

Contact forces are obtained from the calculated overlaps of each component sphere as well as the relative velocities at each contact point. The resulting overall force on the particle is usually determined as

$$\vec{F}_{CP} = \sum_{s=1}^{num} \vec{F}_{s,CSP} \tag{8}$$

With

*num* number of component spheres of the clustered particle

In order to determine contact forces for the component spheres the well known force laws and contact detection schemes can be applied as for regular spherical particles.

The normal overlap of a component sphere can be determined as follows:

Particle–particle collision:

$$\vec{\xi}^{n} = \left(\vec{R}_{j,CSP} + \vec{R}_{k,CSP}\right) - \vec{d}_{AB} \tag{9}$$

Particle–wall collision:

$$\vec{\xi}^{n} = \vec{R}_{j,CSP} - \vec{d}_{AW} \tag{10}$$

With

$j,k$ Indices of the component spheres of particles A and B respectively
$\vec{R}_{CSP}$ Radius of the component spheres
$\vec{d}_{AB}$ Distance between the centres of gravity of particles A and B
$\vec{d}_{AW}$ Distance between the centre of gravity of particle A and the base point on the wall

### 3.2. Polyhedral particles

In order to approximate a specific particle shape with a polyhedral body commercial software can be applied. The basic representation of a polyhedral body is similar to a clustered-particle as outlined in Section 3.1. A global frame of reference and a body-fixed frame have to be employed in order to keep track of translational and rotational body movement. The location $\vec{x}_{j,V}$ of each vertex on the surface can be determined as

$$\vec{x}_{j,V} = \vec{x}_P + M_P \cdot \vec{r}_{j,V} \tag{11}$$

With

$\vec{x}_P$ Position vector of the particle's centre of gravity
$M_P$ Rotational matrix converting vectors from the body-fixed frame to the global coordinate system
$\vec{r}_{j,V}$ Vector from the particle's centre of gravity to the vertex $i$

For the velocity at each vertex of the particle follows

$$\dot{\vec{x}}_{j,V} = \dot{\vec{x}}_P + M_P\left(\vec{\omega}_P \times \vec{r}_{j,V}\right) \tag{12}$$

With

$\vec{\omega}_P$ Rotational velocity of the particle

Detecting contact between polyhedral bodies can be complicated. In scientific literature such as Cundall [13], Nezami et al. [14,36], Zhao et al. [15], and Muth et al. [36] many approaches for the detection of contact between two polyhedral bodies can be found.

Another important issue when dealing with polyhedral bodies is the classification of detected contacts. Contacts between two colliding polyhedral bodies can be classified in vertex-to-vertex, vertex-to-edge, vertex-to-face, edge-to-edge, edge-to-face and face-to-face contacts. As Cundall [13] recognized only vertex-to-face and edge-to-edge contacts need to be checked because all other contact types can be converted into these two contact types.

When only considering vertex-to-face contacts the contact detection between a polyhedral body and a flat wall is quite simple. By calculating the signed distance of each vertex to the flat wall all contacting vertices as well as their overlapping distances with the

wall can be determined. Similar to multi-sphere particles the overall force on the polyhedral body can then be determined as a combination of the contact forces in each contact point. This approach will be used in the investigated collision scenarios in Sections 4 and 5 of this paper.

## 4. Multiple contacts of a multi-sphere with a flat wall

In order to demonstrate the effects of shape approximation on the contact force resolution, a simple particle collision scenario is investigated in the following chapter: a single spherical particle impacting a stationary flat wall at an impact angle α. The sphere is approximated applying a multi-sphere approach with different approximation accuracies. The resulting contact force evolution in normal and tangential direction is compared to the results of a perfect sphere which serves as a reference solution.

### 4.1. Multiple contacts

Studies on multiple contacts occurring during a collision can be found in Kruggel-Emden et al. [7], Kodam et al. [16] and Abbaspour-Fard et al. [28]. Since these studies were carried out for a multi-sphere particle the same approach is chosen for this paper in order to show the limitation of the proposed solutions as well as to provide an improved procedure when dealing with multiple contact collisions.

Modelling a particle's shape with the multi-sphere method the shape approximation shows a certain bumpiness which leads to an artificial roughness of the particle. Kruggel-Emden et al. identified this artificial roughness as limitation of the multi-sphere method when applied to approximate arbitrarily shaped objects [7]. Considering a single particle impacting a flat wall only one contact point will occur if the particle is a perfect rigid sphere. When approximating a sphere with the multi-sphere approach more than one contact point may occur (see Fig. 5). The reason can be found in the fact that the discrete element method allows particles to overlap in order to calculate contact forces based on the overlapping distance. Combined with the multi-sphere approach this leads to a multitude of component spheres contacting the wall depending on the number of component spheres and sphere-orientation during impact. This is even more so if the particle is modelled very soft resulting in larger overlaps. Moreover during the contact period the number of contact points may change abruptly from one iteration step *i* to the next.

The influence of multiple contact points on the mechanical particle behaviour as a result of shape approximation with the multi-sphere approach is outlined in the following.

Recent work by Kruggel-Emden et al. [7] examined the collision of a sphere as well as a sphere-approximation generated with the multi-sphere approach with a stationary flat wall. The orientation of the sphere-approximation as well as its artificial roughness was varied in order to have one, two or three component spheres contacting with the wall during the collision. In particular the orientation of the sphere-approximation was chosen in a way that the resulting overlap of each contacting component sphere was equivalent. Thus the total force acting on the sphere-approximation could be simply divided by the number of contact component spheres. While this approach could be employed in order to show the validity of the multi-sphere approach, it can only do so for this specific collision scenario. In the following it will be demonstrated that for an arbitrary collision of a multi-sphere particle and a wall this approach proves to be insufficient since the overlap at each component sphere is not equal, leading to incorrect contact forces in normal and tangential direction.

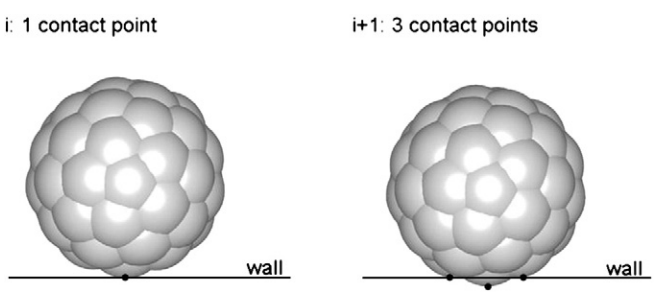


**Fig. 5.** 2D-schematic of a sphere-approximation impacting a flat wall for two different time steps (dots indicating contact points).

Kodam et al. [16] recognized similar to Kruggel-Emden et al. that the calculation of the contact forces has to be adjusted when multiple contacts occur during a collision. In a first step they investigated only the elastic normal force component of a sphere approximated with the multi-sphere method and a stationary flat wall. They stated that the summarized force of the contacting component spheres cannot be equivalent to the contact force of a real sphere impacting the wall as long as the same normal spring stiffness is applied for both cases. Since the number of contacting component spheres is not constant over the collision time, an easy adjustment of the normal spring stiffness is not possible. Instead they recommend modifying the normal spring stiffness and the power exponent ε in the applied force scheme (which is equal to 1 for a linear force scheme) such that the error between the summarized contact force of the component spheres and the reference sphere is minimized. From the results of their studies they conclude that when multiple component spheres make contact, simply using the same spring stiffness for the component spheres as for the real sphere leads to a contact that is too stiff. Moreover they conclude that it is not possible to model contact dissipation a priori for a particle approximated with the multi-sphere method since using a fixed damping coefficient for the component spheres which is equal to the value chosen for the reference sphere would lead to a system with excessive damping. Thus Kodam et al. recommend avoiding velocity-dependent damping when multiple component sphere contacts are expected which presents a considerable limitation of this approach.

In the following section of this paper the effects of multiple contacts on the contact force evolution are illustrated. Moreover an improvement of the current force calculation is provided which reduces the effects of multiple contacts significantly without requiring significant changes in an existing discrete element code.

### 4.2. Effects of the force resolution

Within the multi-sphere method it is a common approach to calculate the contact forces for each contact point and accumulate them in order to determine the cumulative contact force acting on the particle [7,15,16] in each time step. In order to accurately approximate the mechanical behaviour of the actual particle-shape the goal is to have the cumulative force acting on the component spheres equal to the force acting on the “real” particle with the exact shape over the collision period.

Consider the exact same body impacting a flat wall with one and with multiple contact points (as outlined in Fig. 5). With just looking at the elastic component of the normal force $F^{n,el} = k^n \cdot \xi^n$ additional contact points lead to parallel compression (compression phase) or elongation (restitution phase) of the normal spring since the usual linear spring dashpot model is applied to each of the occurring contact points. Assuming the same spring stiffness (as a material property) for a single and multiple contact and just applying Hooke's Law for parallel springs, leads to a higher apparent stiffness of the particle in the case of multiple contacts. This results automatically in a smaller average overlap of the particles for multiple contact points with the consequence of higher values for the deceleration of the particle and, hence, an increase of maximum elastic normal contact force and different contact force evolutions (e.g. shorter time of contact).

The above argumentation makes clear that such a simple approach is not feasible if the same normal force evolution should be reflected for a single and a multiple contact situation. An improved approach has also to keep in mind that:

- the overlap can be different for any of the multiple contact points and that
- the number of contact points can change during the particle impact.

Hence a simple approach like for example adapting spring stiffnesses by dividing the spring stiffness of the single contact by the number of contacts is not a solution of the problem.

Note that in principle a similar argumentation holds true for the dissipative component of the normal force $F^{n,diss} = \gamma^n \cdot \dot{\xi}^n$. Calculating the contact force at $N$ contact points implies the moving of $N$ velocity-dependent dashpots resulting in an overall greater dissipative force component.

The above described contact behaviour does not correspond to physical correct mechanical particle behaviour.

To illustrate the effect of applying the same spring stiffness for multiple and single contacts on the normal force resolution, a DEM-simulation is conducted for the scenario of a sphere and a sphere approximated with a multi-sphere approach colliding with a stationary flat wall. The sphere has a radius of $r = 25$ mm. The sphere-approximation is carried out with 25, 50, 100, 150 and 300 component spheres resulting in a maximum number of contact points ranging from $NCP_{max} = 3$ to $NCP_{max} = 8$. As a rule the number of contacting spheres increases with an increasing number of component spheres in the clustered particle depending also on the impact angle.

For an isolated investigation of the normal force a perpendicular collision with an impact angle of $\alpha = 0°$ (measured from the vertical axis) is selected. The resulting normal force on the clustered particle is calculated in a first step by simple adding of the component forces at each contact point.

Fig. 6 shows the according normal force evolution of the sphere–wall collision.

Fig. 6 shows a significant difference of the force evolutions for the clustered particle to the reference solution of the perfect sphere. The sphere approximations show a much higher maximum normal force as well as a considerably shorter contact time. Moreover the corresponding curves show irregular lapses which indicate that the number of contact points changes during the collision resulting in a sudden increase or decrease of the overall normal force acting on the particle. Moreover the deviation from the reference solution increases with an increasing number of component spheres and thus with an increasing number of contact points.

Fig. 7 shows the force evolution curves for the normal and tangential direction for the same collision scenario with an impact angle of $\alpha = 45°$. The chosen impact angle results in significant tangential forces acting during the particle-wall contact and therewith allows investigation of the effect of multiple contacts on the tangential force evolution as well.

Again the contact forces in normal as well as in tangential direction for the sphere-approximation have a significant higher maximum value while the contact time is smaller when compared to the reference solution of the perfect sphere. Moreover the deviation from the reference solution increases with an increasing number of component spheres and therewith contact points. Testing has shown that reducing the time step size of the iteration does neither change the occurrence of the observed leaps in the force evolution nor does it significantly reduce the absolute deviation from the results of the perfect sphere impacting the wall.

Due to the tremendous effect of multiple contacts on the contact force resolution, a DEM-simulation has to account for this scenario in order to obtain correct mechanical particle behaviour. A possible solution as demonstrated by Kruggel-Emden et al. [7] would be to calculate the mean value of the component contact forces, i.e. divide the summarized component forces at iteration step $i$ by the number of contact points at $i$. For the particular case of an equivalent contact force at each contact point, this solution would provide accurate results as demonstrated in Ref. [7]. For the more general case, which is investigated in this paper, this solution proposal leads to a large deviation from the reference solution as well (see Fig. 8) and therefore has to be rejected.

In modern DEM-Codes the calculation of normal contact forces is carried out for each iteration step [12,30–32]. In comparison to an incremental approach of determining contact forces this avoids the possibility of accumulating numerical deviations as well as it reduces memory requirements since contact forces from previous iteration steps do not have to be stored in the working memory.

As Kodam et al. showed it is not possible to adjust the normal spring stiffness of the contacting particle directly when more than one contact point is involved in the collision. Nevertheless the necessary adjustment is easy to achieve when applying an incremental approach to determine contact forces.

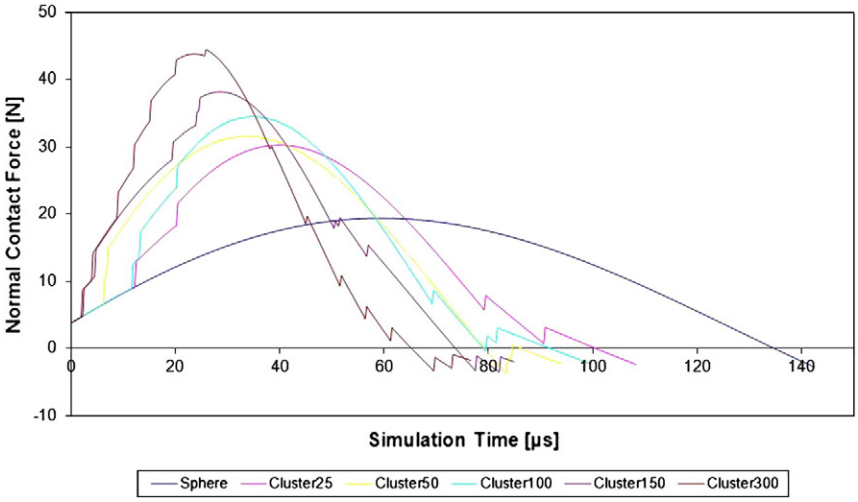


**Fig. 6.** Normal force evolution of a particle-wall contact with an impact angle $\alpha = 0°$ for a spherical particle compared to an approximated sphere with the multi-sphere approach (comprising 25, 50, 100, 150 and 300 component spheres).

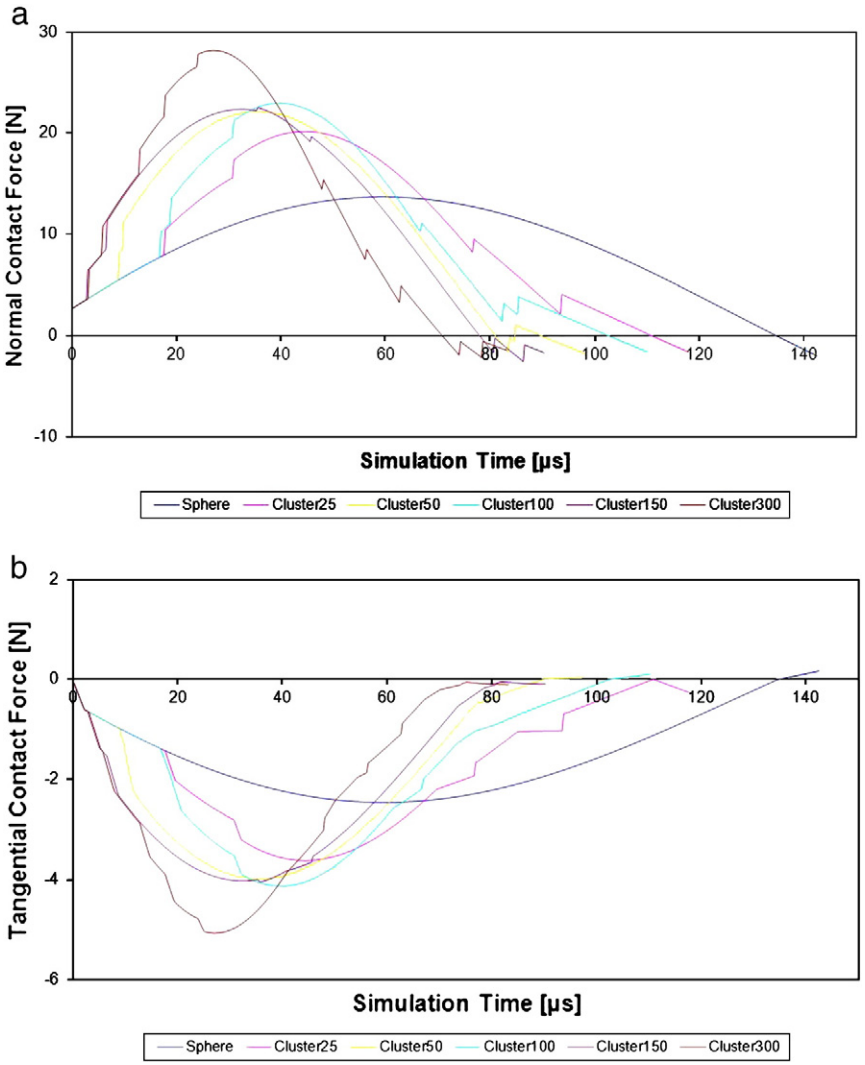


**Fig. 7.** a) Normal and b) tangential force evolution of a particle-wall contact with an impact angle $\alpha = 45°$ for a spherical particle compared to an approximated sphere with the multi-sphere approach (comprising 25, 50, 100, 150 and 300 component spheres).

Incremental approach:

$$F_i^n = F_i^{n,el} + F_i^{n,diss} = \left(F_{i-1}^{n,el} + \Delta F_i^{n,el}\right) + \left(F_{i-1}^{n,diss} + \Delta F_i^{n,diss}\right). \tag{13}$$

With the incremental elastic normal force for the current iteration step $i$:

$$\Delta F_i^{n,el} = k^n \cdot \Delta \xi_i^n. \tag{14}$$

Where

$$\Delta \xi_i^n = \xi_i^n - \xi_{i-1}^n. \tag{15}$$

And the dissipative normal force for the current iteration step:

$$F_i^{n,diss} = \gamma^n \cdot \Delta \dot{\xi}_i^n. \tag{16}$$

Where

$$\Delta \dot{\xi}_i^n = \dot{\xi}_i^n - \dot{\xi}_{i-1}^n. \tag{17}$$

Thus for multiple contact points the two incremental force elements can be determined as

$$\Delta F_i^{n,el} = \frac{1}{NCP}\sum_{s=1}^{NCP} \Delta F_{i,s}^{n,el} = \frac{k^n}{NCP}\sum_{s=1}^{NCP} \Delta \xi_{i,s}^n \tag{18}$$

and

$$\Delta F_i^{n,diss} = \frac{\gamma^n}{NCP}\sum_{s=1}^{NCP} \Delta \dot{\xi}_{i,s}^n. \tag{19}$$

For the sake of comparison Eqs. (20a) and (20b) show the conditional equations of the normal contact force using the normal approach (a) as well as an incremental approach (b) as derived in this section:

$$F_i^n = F_i^{n,el} + F_i^{n,diss} = \frac{k^n}{NCP}\sum_{s=1}^{NCP} \xi_{i,s}^n + \frac{\gamma^n}{NCP}\sum_{s=1}^{NCP} \dot{\xi}_{i,s}^n \tag{20a}$$

$$F_i^n = F_i^{n,el} + F_i^{n,diss} = F_{i-1}^{n,el} + \frac{k^n}{NCP}\sum_{s=1}^{NCP}\left(\xi_{i,s}^n - \xi_{i-1,s}^n\right) + F_{i-1}^{n,diss} + \frac{\gamma^n}{NCP}\sum_{s=1}^{NCP}\left(\dot{\xi}_{i,s}^n - \dot{\xi}_{i-1,s}^n\right). \tag{20b}$$

By calculating the elastic and dissipative normal contact force incrementally and dividing only the incremental force elements by

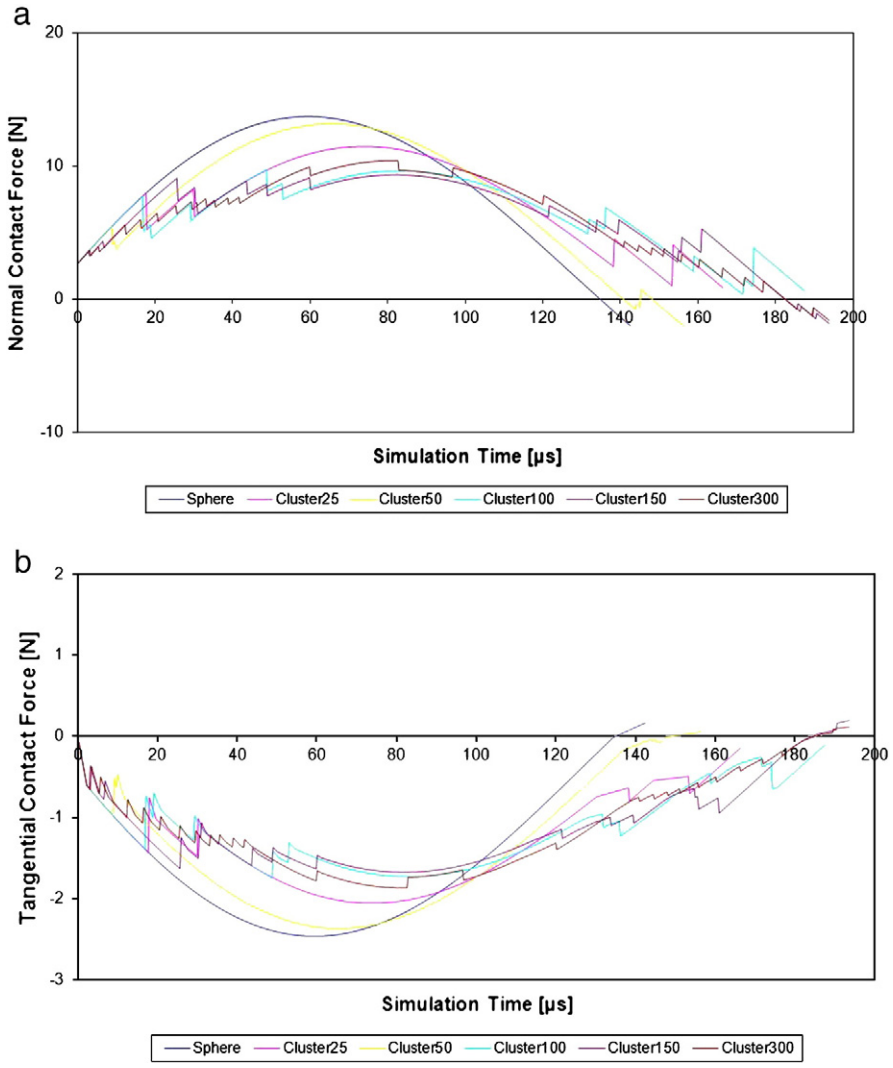


**Fig. 8.** a) Normal and b) tangential force evolution of a particle-wall contact with an impact angle $\alpha = 45°$ for a spherical particle compared to an approximated sphere with the multi-sphere approach. The overall contact force on the clustered particle is divided by the number of contact points.

the number of the contact points in the current iteration step *i*, the effect of compressing/elongating multiple springs as well as moving multiple dashpots can be modified in a way that it corresponds to the single contact behaviour of a perfect sphere. Dividing only the accruing incremental force elements by the number of contact points accounts for the changing number of contacts during the collision process. Since new contact points must not necessarily occur exactly at the beginning of an iteration step and existing contact points must not necessarily vanish at the end of an iteration step, the contact force calculation above described still leads to minor deviations from the normal force evolution of a single contacting sphere. Tests have shown that the deviations can be further reduced through selection of a sufficiently small enough time step.

Fig. 9 shows the previously investigated scenario of a sphere and a sphere-approximation impacting a flat wall with an impact angle $\alpha_1 = 0°$ and $\alpha_2 = 45°$. This time the normal contact force is determined incrementally as outlined in Eqs. (13)–(17).

The improvement in terms of reducing deviations between the normal contact force evolution of a perfect sphere and sphere-approximation is evident comparing Fig. 9a)–b) with Figs. 6–8.

An adaptation of the tangential force calculation is carried out analogously to the normal force calculation. Since the tangential force according to Eq. (4) can switch between the Coulomb force $F^{t,coul}$ and the tangential spring force $F^{t,tspg}$ an adaptation of the tangential spring is recommended instead of adjusting the tangential forces directly.

$$\xi_i^t = \xi_{i-1}^t + \frac{v_i^t \cdot dt}{NCP}. \tag{21}$$

Additionally vanishing of existing contact points has to be accounted for when calculating tangential forces since in contrast to the normal spring elongation $\xi^n$, the tangential spring elongation $\xi^t$ does not necessarily return to 0 before the contact ends. Tests have shown that without any adaptation ceasing of existing contact points would lead to unphysical leaps in the tangential contact force evolution. For this reason the tangential spring elongation of ceasing contact points is distributed equally on the tangential spring elongations of the other still existing contact points. The distribution of the tangential spring elongation is only a mean to conserve the overall tangential force when a contact ends. The energy balance is not violated since the overall spring force as well as the overall overlap of the contact remains unchanged while only the component tangential forces in each of the remaining contact points increase in order to compensate the 'loss' of tangential force due to the ceasing of a contact point.

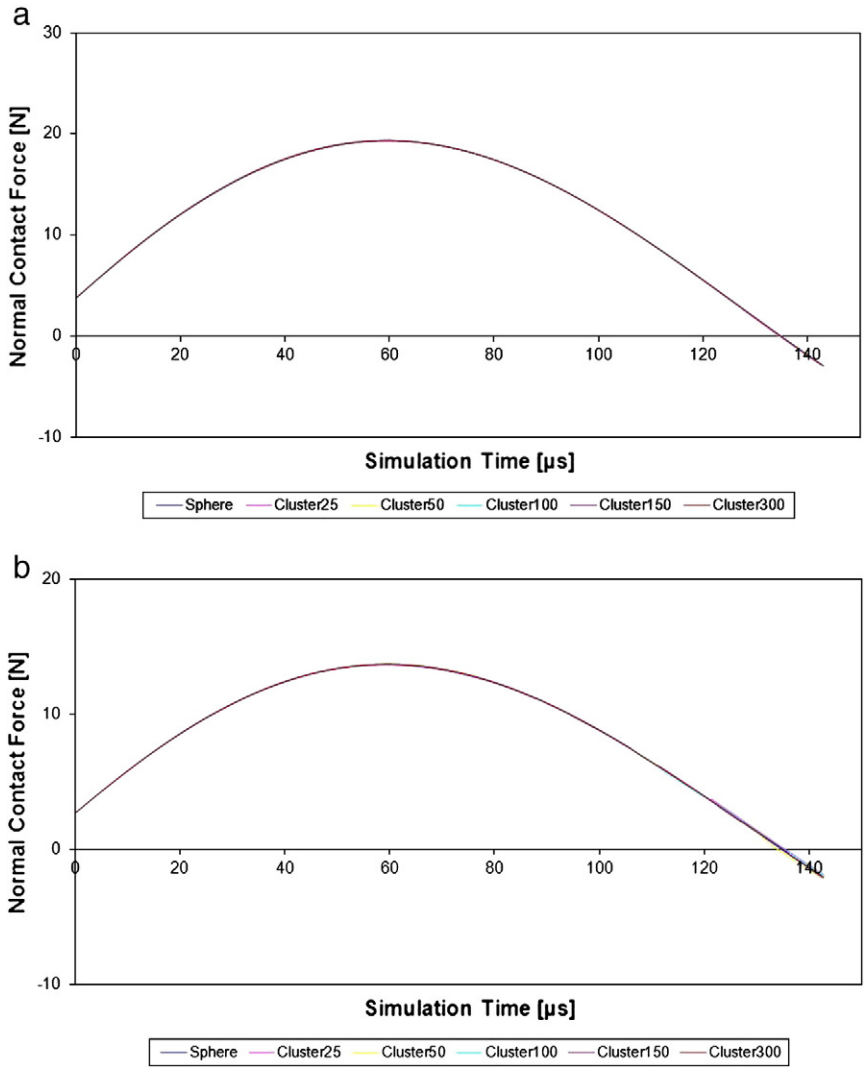


**Fig. 9.** Normal force evolution of a particle-wall collision for an impact angle of a) $\alpha_1 = 0°$ and b) $\alpha_2 = 45°$.

Implementing the above specified adjustments to the tangential force calculation leads to the following results for the investigated particle-wall collision.

While the approximated solution of the normal force evolution matches the reference solution perfectly, there are still some minor deviations when investigating the tangential forces (Fig. 10). These deviations may either be caused by the different surface structures of the clustered particle when compared to a perfect sphere or they may be induced by the multiple contacts occurring during the collision. The absolute deviations of the tangential contact force averaged over the full contact time for the 5 investigated approximation accuracies are summarized in Table 2.

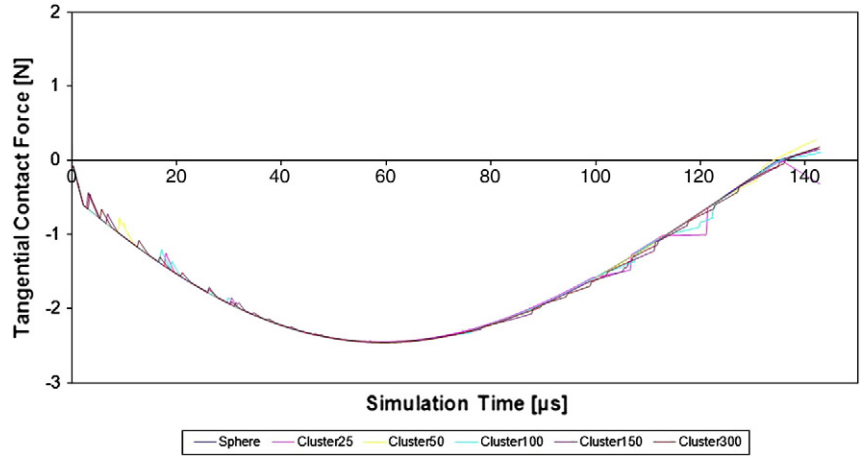


**Fig. 10.** Tangential force evolution of a particle-wall collision for an impact angle of $\alpha = 45°$.

**Table 2**
Averaged deviation of the tangential contact force for the 5 investigated approximation accuracies.

| | CP25 | CP50 | CP100 | CP150 | CP300 |
|---|---|---|---|---|---|
| Averaged deviation [N] | 0.0285 | 0.01284 | 0.0200 | 0.0202 | 0.0215 |

The results show that an increase in component spheres and thus increase of the sphere-surface approximation accuracy does not automatically lead to more accurate results. In contrast the approximation with 50 CSP shows by far the best results in the test series. Obviously the effect of a better particle surface approximation induced by an increasing number of component spheres is annihilated or even overcompensated by the effect of multiple contacts on the tangential force calculation.

## 5. Comparison of multi-sphere and polyhedral approaches

### 5.1. Similarities between both approaches

A multi-sphere particle impacting a flat wall may have multiple contact points, i.e. component spheres in contact with the wall, according to its impact angle and initial rotation. As explained in Section 3.1 of this paper, for each contact point the contact forces are calculated based on the local overlap as well as the local relative velocity. The resulting force on the particle can be determined by combining all component forces (see Eq. (8)).

As described in Section 3.2 contacts between two polyhedral bodies can be differentiated into two different contact types, that is vertex-to-face and edge-to-edge contact. Investigating the impact of a polyhedral body on the centre of a flat wall, only vertex-to-face contacts need to be checked because an edge-to-edge contact is not possible. Calculating the contact force for a vertex-to-face contact is straightforward as it is similar to a sphere-wall contact. In summary the contact forces resulting from a collision between a polyhedral body and a flat wall can be calculated by determining the respective vertex-to-face contacts and calculate the contact forces at each contact point before combining them to the resulting overall force acting on the particle.

So in fact this is the same procedure that is carried out for a multi-sphere cluster-particle impacting a wall which makes a direct comparison of both approaches possible.

### 5.2. Ellipsoid-wall collision scenario

In this section of the paper an ellipsoidal particle impacting a flat stationary wall is investigated as shown in Fig. 11. Contact properties are derived using the common normal concept as introduced by Lin and Ng [9]. In this contact detection scheme two points, one on each ellipsoid surface, are iteratively determined in a way that the outward normal vectors in each point as well as the straight line connecting both points are parallel. In the case of an ellipsoid impacting a flat wall the contact detection scheme reduces to finding the point on the ellipsoid-surface in which the outward normal vector is parallel to the normal vector of the flat wall. Since two surface-points will meet this criterion the one with the shorter distance to the wall is selected.

For the sake of comparison the results calculated for normal and tangential forces as well as the rebound angle obtained by using the common normal concept are denoted as reference solution.

The ellipsoid is approximated with a multi-sphere approach as well as with the polyhedral approach. The same material properties are used in the simulation as for the sphere-wall contact as summarized in Table 1.

For the multi-sphere approximation of the ellipsoid an algorithm similar to the one developed by Markauskas et al. [8] is applied

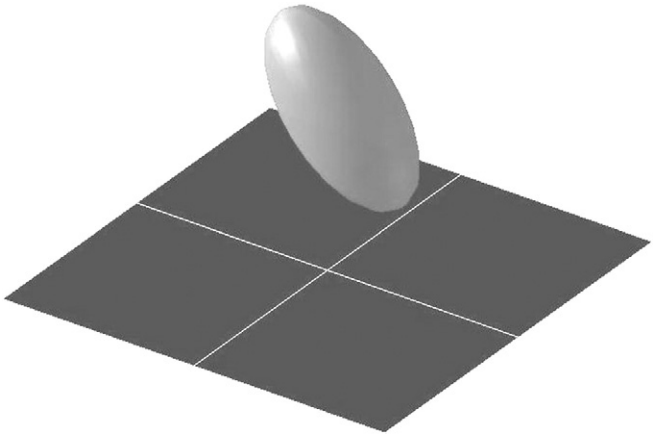

**Fig. 11.** Ellipsoidal particle impacting a stationary flat wall.

because it allows a good approximation of the ellipsoidal body with relatively small numbers of inscribed spheres. In the algorithm spheres are inscribed into a given ellipsoid with the centre of the spheres located on its largest axis. The distance between the neighbouring spheres is equal and their radiuses are chosen in a way that at each contact point of sphere and ellipsoid a tangential plane can be constructed (compare to Section 3.1). Fig. 12 gives an example of the ellipsoid-approximations for varying accuracies.

The results of both approximation procedures at different approximation levels for various collision scenarios are compared with the reference solution of the actual ellipsoid. The applicability of multi-sphere and polyhedral approaches for approximating ellipsoidal particles is discussed.

In the investigated collision scenario an ellipsoidal particle is colliding with a flat wall at an impact angle of 0° with particle rotations ranging from 0 to 90° where at a rotation angle of 90° the long axis of the ellipsoid is perpendicular to the wall surface. Fig. 13a and b shows the deviation of the normal contact force averaged over contact time as a percentage of the reference solution.

Mean values of the normal force deviations over particle rotations ranging from 0 to 90° with regard to the averaged normal force of the investigated ellipsoid-approximations are summarized in Table 3.

The results show an increase of the averaged deviation for the multi-sphere approximation with increasing approximation accuracy, i.e. increasing number of component spheres. On the other hand the averaged deviation for the polyhedral ellipsoid-approximation ranging from 25 to 200 vertices is almost constant with CL100 yielding the most accurate results. Poly15 comprising 15 vertices shows by far the highest deviations of the polyhedral ellipsoid-approximations. Obviously a certain amount of vertices is necessary in order to adequately approximate an ellipsoidal particle shape.

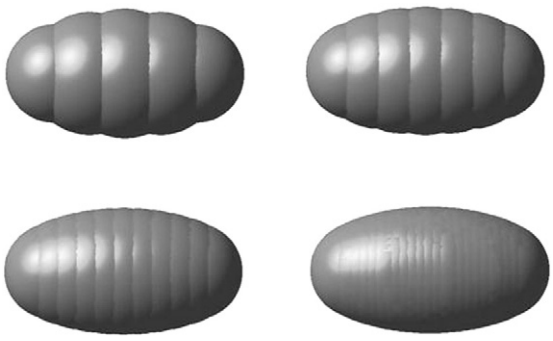

**Fig. 12.** Ellipsoid-approximations using a multi-sphere approach with varying levels of shape-approximation accuracy.

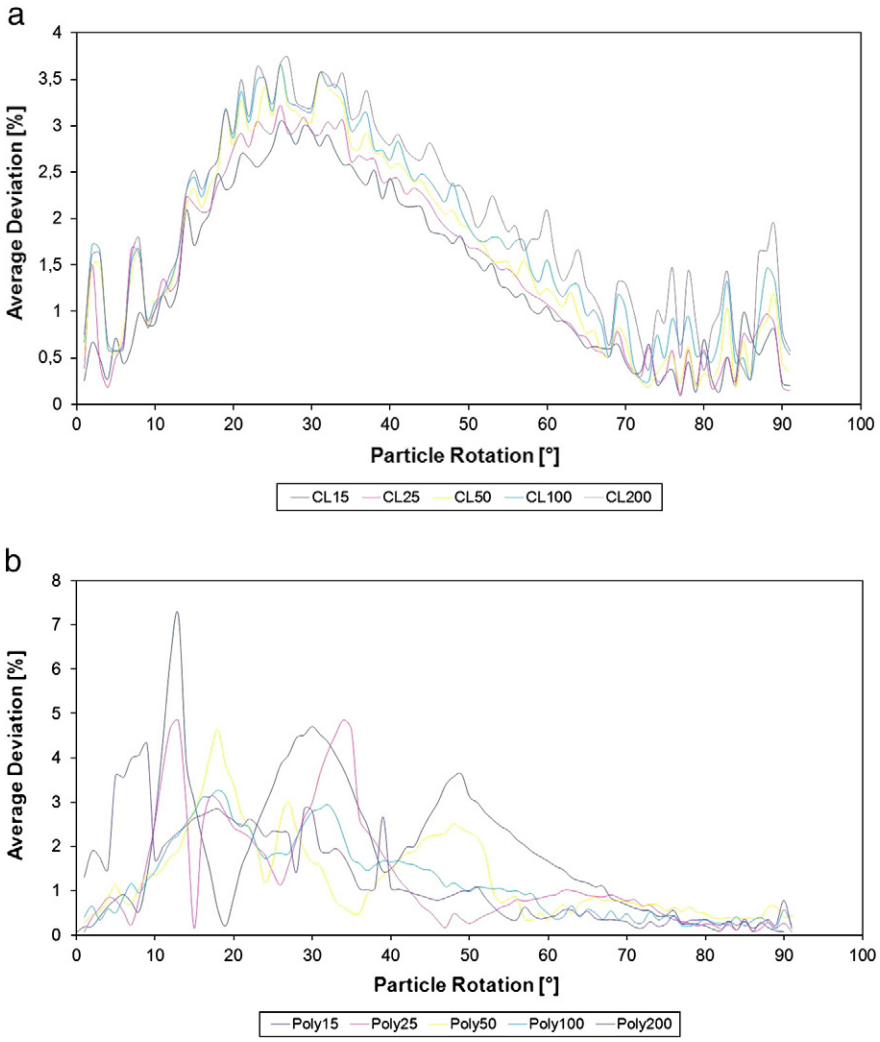


**Fig. 13.** Percentaged deviation of the normal force averaged over contact time for the a) multi-sphere approximation and b) polyhedral approximation.

A possible cause for this surprising behaviour can be deduced when looking at the average number of contact points over the collision time (see Table 4).

Naturally the number of contact points increases with an increasing number of component spheres or polyhedron vertices. Nevertheless it happens that the number of contact points of the multi-sphere approximation increases in the investigated collision scenario much faster than for the polyhedral approximation. Thus the effect of multiple contacts on the force resolution as described in Section 4 of this paper influences the multi-sphere approximation much more than the polyhedral one. Obviously the sharp increase of contact points for the multi-sphere approximation overcompensates the positive effect of a more accurate ellipsoid-surface approximation. On the other hand, the polyhedral approximation shows a minimum normal force deviation for 100 vertices. This specific approximation seems to result in the best compromise between the two effects of accurate surface-approximation and number of contact points. It should be noted at this point that the increase in the number of contact points with increasing shape-approximation accuracy depends considerably on the applied shape-approximation algorithm.

Similar results can be obtained from investigating the tangential contact forces of the ellipsoid impacting the wall (Fig. 14).

Mean values of the tangential force deviations over particle rotations ranging from 0 to 90° with regard to the averaged tangential force of the investigated ellipsoid-approximations are summarized in Table 5.

Again an improved shape-approximation of the multi-sphere method results in larger deviations from the reference solution. On the other hand the polyhedral approximation comprising 50 vertices yields the best results in the polyhedral test series. Notice that the deviation of the tangential forces from the reference solution in

**Table 3**
Percentaged deviation of the normal force from the reference solution averaged over the investigated particle rotations for the multi-sphere and polyhedral ellipsoid-approximations.

| | CL15 | CL25 | CL50 | CL100 | CL200 |
|---|---|---|---|---|---|
| Average deviation [%] | 1.384 | 1.511 | 1.646 | 1.792 | 1.956 |
| | Poly15 | Poly25 | Poly50 | Poly100 | Poly200 |
| Average deviation [%] | 1.864 | 1.309 | 1.299 | 1.201 | 1.213 |

**Table 4**
Average number of contact points during a collision for both investigated ellipsoid-approximation approaches.

| | CL15 | CL25 | CL50 | CL100 | CL200 |
|---|---|---|---|---|---|
| Average number of contact points | 3.98 | 6.26 | 12.60 | 24.77 | 48.77 |
| | Poly15 | Poly25 | Poly50 | Poly100 | Poly200 |
| Average number of contact points | 1.35 | 1.96 | 3.09 | 7.78 | 12.89 |

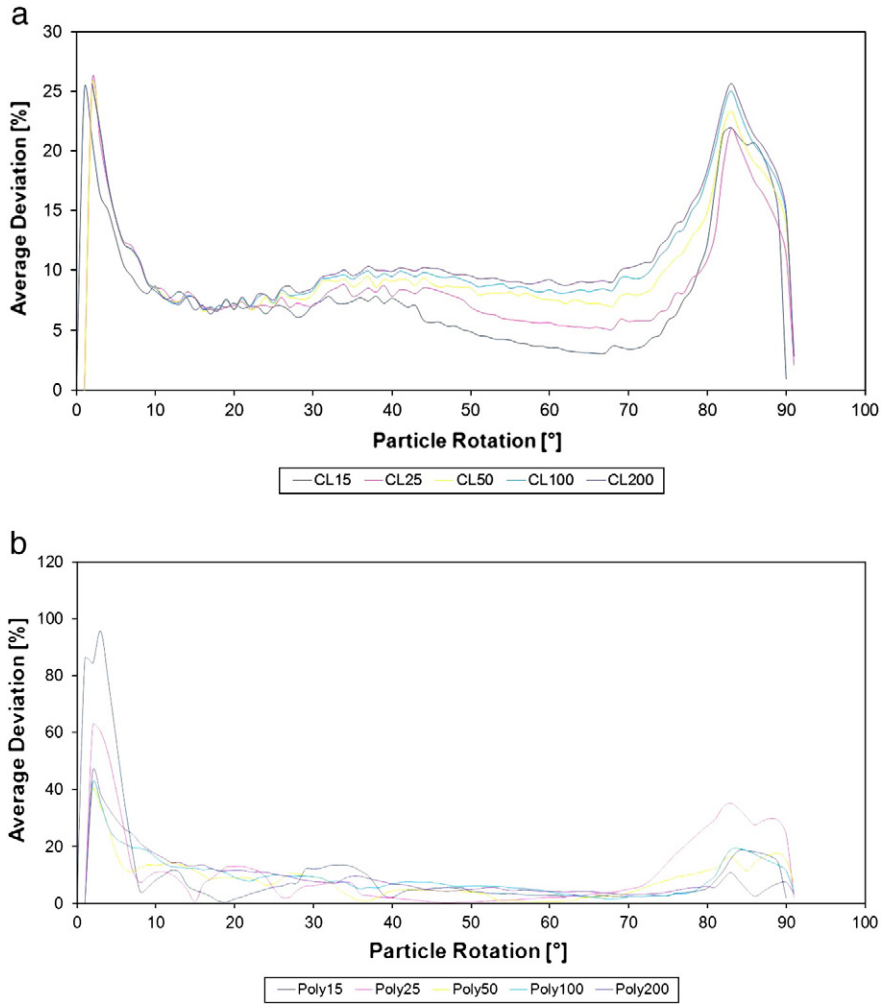


**Fig. 14.** Percentaged deviation of the tangential force averaged over the contact time for the a) multi-sphere approximation and b) polyhedral approximation.

average is much higher than for the normal forces. This is largely caused by high deviations for particle rotations near 0° and 90° resulting in very small tangential forces. Small differences of the surface structure may lead to minor absolute tangential force deviations which in turn are huge percentagewise. Over a large range of rotation angles the deviations are nevertheless in the area of single-digit percentage with the tangential force being considerably smaller than the normal force component.

To further evaluate the adequacy of the multi-sphere and polyhedral approach for approximating ellipsoidal particles as well as the quality of the results for different approximation accuracies, the resulting rebound angle of the particle-wall collision is investigated in the following. Table 6 summarizes the averaged deviation of the rebound angles from the reference solution.

The resulting deviations of the rebound angles confirm the conclusions drawn from investigating the force calculation results. Moreover both approximation procedures at any investigated accuracy level result in rebound angle deviations ranging from roughly 1–3%. In order to confirm the adequacy of both approximation procedures for ellipsoidal particles these deviations can be considered acceptable.

### 5.3. Comparison of the average calculation time

Although calculation time always strongly depends on the implementation of the specific algorithm a rough estimation of the CPU requirements of the two approximation procedures in comparison with the ellipsoid can be given.

**Table 5**
Percentaged deviation of the tangential force from the reference solution averaged over the investigated particle rotations for the multi-sphere and polyhedral ellipsoid-approximations.

| | CL15 | CL25 | CL50 | CL100 | CL200 |
|---|---|---|---|---|---|
| Average deviation [%] | 7.99 | 8.78 | 10.03 | 10.88 | 11.29 |
| | Poly15 | Poly25 | Poly50 | Poly100 | Poly200 |
| Average deviation [%] | 10.77 | 11.16 | 8.21 | 9.37 | 9.09 |

**Table 6**
Deviation of the rebound angle from the reference solution averaged over the investigated particle rotations ranging from 0 to 90° for the multi-sphere and polyhedral ellipsoid-approximations.

| | CL15 | CL25 | CL50 | CL100 | CL200 |
|---|---|---|---|---|---|
| Averaged deviation [%] | 1.04 | 1.25 | 1.32 | 1.36 | 1.50 |
| | Poly15 | Poly25 | Poly50 | Poly100 | Poly200 |
| Averaged deviation [%] | 2.75 | 2.11 | 1.02 | 1.13 | 1.05 |

**Table 7**
Calculation time of the multi-sphere and polyhedral ellipsoid-approximation impacting a flat wall as percentage of the reference solution of the ellipsoid.

| | CL15 | CL25 | CL50 | CL100 | CL200 |
|---|---|---|---|---|---|
| Calculation time [%] | 6.44 | 7.75 | 10.95 | 17.38 | 29.84 |
| | Poly15 | Poly25 | Poly50 | Poly100 | Poly200 |
| Calculation time [%] | 7.56 | 10.20 | 15.33 | 27.25 | 47.95 |

Table 7 shows that both the multi-sphere as well as the polyhedral ellipsoid-approximation requires on average significant less calculation time than the ellipsoid-algorithm.

Especially the approximation at low to medium accuracy levels of both approximation procedures result in large reductions of the calculation time while still yielding acceptable results. It is worth noticing that the polyhedral approximation requires more calculation time than the multi-sphere ellipsoid at the same accuracy level since the contact detection between a vertex and a flat wall is slightly more time consuming than between a component sphere and a wall.

## 6. Summary

When implementing more complex body shapes such as polyhedra and multi-sphere cluster into a discrete element code multiple contact points may occur during a collision. A collision scenario incorporating a spherical particle colliding with a stationary flat wall was investigated in this paper. The spherical particle shape was approximated using a multi-sphere approach. For both the normal and tangential directions a linear viscoelastic force scheme, comprising of a spring and a dashpot, was selected. Consideration of the contact force evolution in both directions shows considerable deviations from the exact solution for the shape approximation-scheme. While a perfect sphere can only have single contact collisions, the sphere-approximation may very well show multiple contacts depending on the accuracy of the shape approximation procedure as well as the orientation of the sphere-approximation and its stiffness. If not implemented correctly these multiple contacts may lead to a non-physical collision behaviour between discrete elements and may therefore result in less accurate DEM simulations.

As outlined in this paper the correct sequence of calculation steps in the contact force calculation is required in order to reduce the effect of multiple contacts in a collision. These adjustments are easy to implement and lead to more accurate solutions of the contact force evolution in normal and tangential direction. While the deviations in normal direction caused by multiple contacts could be annihilated almost totally applying the described adjustments, the deviations in tangential direction could only be reduced to a certain degree.

In a next step the collision of an ellipsoidal particle as well as its approximation using a multi-sphere and a polyhedral approach with a stationary flat wall was investigated. For both approximation procedures higher accuracy levels do not automatically lead to more accurate results. It was shown that the effects of a more accurate ellipsoid-surface approximation and higher numbers of contact points may influence the quality of the results in opposite directions. A compromise between the two effects at medium levels of approximation-accuracy yielded the best results.

The adequacy of the multi-sphere and polyhedral approach to approximate particle-wall collisions of ellipsoidal particles was demonstrated. Both approaches required significant smaller computing times/computational effort compared to the ellipsoid contact algorithm while still yielding acceptable results. Thus based on the results of the investigated collision scenario both procedures can be considered an adequate and promising alternative to implementing ellipsoids in a discrete element code.

The results presented in this paper give an important indication about how geometry in a general DEM simulation can influence the contact force evolution. Before a final conclusion can be drawn more approximation schemes as well as larger particle systems should be examined. This would allow evaluating and quantifying the overall effect of multiple contacts on a particle system and their importance for discrete element simulations.

## Acknowledgement

The current study has been funded by the German Science Foundation (DFG) within the project SCHE 322/6-1. The authors would like to acknowledge the generous support.

## References

[1] H. Kruggel-Emden, E. Simsek, S. Rickelt, S. Wirtz, V. Scherer, Review and extension of normal force models for the Discrete Element Method, Powder Technology 171 (3) (2007) 157–173.
[2] F.P. Di Maio, A. Di Renzo, Analytical solution for the problem of frictional-elastic collisions of spherical particles using the linear model, Chemical Engineering Science 59 (16) (2004) 3461–3475.
[3] H. Kruggel-Emden, S. Wirtz, V. Scherer, A study on tangential force laws applicable to the discrete element method (DEM) for materials with viscoelastic or plastic behaviour, Chemical Engineering Science 63 (6) (2008) 1523–1541.
[4] A. Di Renzo, F.P. Di Maio, Comparison of contact-force models for the simulation of collision in DEM-based granular flow codes, Chemical Engineering Science 59 (2004) 525–541.
[5] J.P. Latham, A. Munjiza, The modelling of particle systems with real shapes, Philosophical Transactions of The Royal Society of London, Series A: Mathematical Physical and Engineering Sciences 362 (1822) (2004) 1953–1972.
[6] H. Kruggel-Emden, S. Wirtz, V. Scherer, Applicable contact force models for the discrete element method: the single particle perspective, Journal of Pressure Vessel Technology 131 (2) (2009) 024001.
[7] H. Kruggel-Emden, S. Rickelt, S. Wirtz, V. Scherer, A study on the validity of the multi-sphere Discrete Element Method, Powder Technology 188 (2) (2008) 153–165.
[8] D. Markauskas, R. Kacianauskas, A. Dziugys, R. Navakas, Investigations of adequacy of multi-sphere approximation of elliptical particles for DEM simulations, Granular Matter 12 (1) (2010) 107–123.
[9] X.S. Lin, T.T. Ng, Contact detection algorithms for 3-dimensional ellipsoids in discrete element modelling, International Journal for Numerical and Analytical Methods in Geomechanics 19 (9) (1995) 653–659.
[10] H. Ouadfel, L. Rothenburg, An algorithm for detecting inter-ellipsoid contacts, Computers and Geotechnics 24 (4) (1999) 245–263.
[11] P.W. Cleary, N. Stokes, J. Hurley, Efficient collision detection for three-dimensional super-ellipsoidal particles, Computational Techniques and Applications: CSIRO Division of Mathematical and Information Science 1997, Clayton, Australia, 1997.
[12] P.W. Cleary, M.L. Sawley, DEM modelling of industrial granular flows: 3D case studies and the effect of particle shape on hopper discharge, Applied Mathematical Modelling 26 (2) (2002) 89–111.
[13] P.A. Cundall, Formulation of a three-dimensional distinct element model — part 1. a scheme to detect and represent contacts in a system composed of many polyhedral blocks, International Journal of Rock Mechanics and Mining Sciences 25 (3) (1988) 107–116.
[14] E.G. Nezami, Y.M.A. Hashash, J. Ghaboussi, D. Zhao, A fast contact detection algorithm for discrete element method, 16th ASCE Engineering Mechanics Conference July 16–18 2003, University of Washington, Seattle, 2003.
[15] D. Zhao, E.G. Nezami, Y.M.A. Hashash, J. Ghaboussi, Three-dimensional discrete element simulation for granular materials, International Journal for Computer-Aided Engineering and Software 23 (7) (2006) 749–770.
[16] M. Kodam, R. Bharadwaj, J. Curtis, B. Hancock, C. Wassgren, Force model considerations for glued-sphere discrete element method simulations, Chemical Engineering Science 64 (15) (2009) 3466–3475.
[17] H. Abou-Chakra, J. Baxter, U. Tuzun, Three-dimensional particle shape descriptors for computer simulation of non-spherical particulate assemblies, Advanced Powder Technology 15 (1) (2004) 63–77.
[18] C. Hogue, Shape representation and contact detection for discrete element simulations of arbitrary geometries, Engineering Computations 15 (3) (1996) 374–390.
[19] J.M. Ting, B.T. Corkum, Strength behaviour of granular materials using discrete numerical modelling, Proceedings 6th International Conference on Numerical Methods in Geomechanics, vol. 1, Innsbruck, Austria, 1988, pp. 305–310.
[20] X. Lin, T.T. Ng, A three-dimensional discrete element model using arrays of ellipsoids, Geotechnique 47 (2) (1997) 319–329.
[21] A. Dziugys, B. Peters, A new approach to detect the contact of two-dimensional elliptical particles, International Journal for Numerical and Analytical Methods in Geomechanics 25 (15) (2001) 1487–1500.
[22] L. Rothenburg, R.J. Bathurst, Numerical simulation of idealized granular assemblies with plane elliptical particles, Computers and Geotechnics 11 (4) (1991) 315–329.

[23] E. Azéma, F. Radjai, R. Peyroux, V. Richefeu, G. Saussine, Short-time dynamics of a packing of polyhedral grains under horizontal vibrations, European Physical Journal E: Soft Matter and Biological Physics 26 (3) (2008) 327–335.
[24] J. Ghaboussi, R. Barbosa, Three-dimensional discrete element method for granular materials, International Journal for Numerical and Analytical Methods in Geomechanics 14 (7) (1990) 451–472.
[25] J.F. Favier, M.H. Abbaspour-Fard, M. Kremmer, A.O. Raji, Shape representation of axi-symmetrical, non-spherical particles in discrete element simulations using multi-element particles, Engineering Computations 16 (4) (1999) 467–480.
[26] M.H. Abbaspour-Fard, Discrete element modelling of the dynamic behaviour of non-spherical particulate materials, PhD Thesis (2001), University of Newcastle upon Tyne, UK.
[27] X. Garcia, J.P. Latham, J. Xiang, J. Harrison, A clustered overlapping sphere algorithm to represent real particles in distinct element modelling, Geotechnique 59 (9) (2009) 779–784.
[28] M.H. Abbaspour-Fard, Theoretical validation of a multi-sphere, discrete element model suitable for biomaterials handling simulation, Biosystems Engineering 88 (2) (2004) 153–161.
[29] H. Kruggel-Emden, Analysis and improvement of the time-driven discrete element method, PhD Thesis (2008), Shaker Verlag.
[30] Y. Tsuji, T. Kawaguchi, T. Tanaka, Discrete particle simulation of two-dimensional fluidized bed, Powder Technology 77 (1) (1993) 79–87.
[31] S. Limtrakul, A. Boonsrirat, T. Vatanatham, DEM modelling and simulation of a catalytic gas–solid fluidized bed reactor: a spouted bed as a case study, Chemical Engineering Science 59 (22–23) (2004) 5225–5231.
[32] H. Kruggel-Emden, E. Simsek, S. Wirtz, V. Scherer, Modelling of granular flow and combined heat transfer in hoppers by the discrete element method (DEM), Journal of Pressure Vessel Technology 128 (3) (2006) 439–444.
[33] L. Brendel, S. Dippel, Lasting contacts in molecular dynamics simulations, in: H. Herrmann, J.P. Hovi, S. Luding (Eds.), Physics of Dry Granular Media, Kluwer Academic Publishers, Dordrecht, 1998.
[34] F.P. Di Maio, A. Di Renzo, Analytical solution for the problem of frictional-elastic collisions of spherical particles using the linear model, Chemical Engineering Science 59 (16) (2004) 3461–3475.
[35] P.A. Cundall, O.D.L. Strack, A discrete numerical model for granular assemblies, Geotechnique 29 (1979) 47–65.
[36] B. Muth, G. Of, P. Eberhard, O. Steinbach, Collision detection for complicated polyhedra using the fast multipole method or ray crossing, Archive of Applied Mechanics 77 (7) (2007) 503–521.
[37] E.G. Nezami, Y.M.A. Hashash, D. Zhao, J. Ghaboussi, Shortest link method for contact detection in discrete element method, International Journal for Numerical and Analytical Methods in Geomechanics 30 (8) (2006) 783–801.